NASA TM X-609

Declassified by authority of NASA diessification Change Notices No. 17/

N80K-00

TECHNICAL MEMORANDUM

X-609

TRANSONIC WIND-TUNNEL MEASUREMENTS OF THE DAMPING IN PITCH AND OSCILLATORY LONGITUDINAL STABILITY OF SEVERAL REENTRY VEHICLES HAVING LOW LIFT-DRAG RATIOS By Robert A. Kilgore and William C. Hayes, Jr.

> Langley Research Center Langley Air Force Base, Va.

		AUTHOR (T	
NG9 - 7	(CODE)	ine Proposition of Signed H. G.	ng & Delam Yainaa Code Bi
(NASA CR OR TMX OR AD NUMBER)	(CATEGORY)		

NATIONAL AERONAUTICS AND SPACE ADMINISTRATION October 1961 WASHINGTON



TECHNICAL MEMORANDUM X-609

TRANSONIC WIND-TUNNEL MEASUREMENTS OF THE

DAMPING IN PITCH AND OSCILLATORY LONGITUDINAL STABILITY

OF SEVERAL REENTRY VEHICLES HAVING LOW LIFT-DRAG RATIOS*

By Robert A. Kilgore and William C. Hayes, Jr.

SUMMARY

Wind-tunnel measurements of the damping in pitch and oscillatory longitudinal stability of several reentry bodies having low lift-drag ratios have been made by using a forced-oscillation technique. The configurations tested were three high-drag axisymmetric bodies (identified as configurations I-2C, I-2G, and I-2F), a blunt body of revolution with an asymmetric afterbody (configuration I-2), and a blunted cone (configuration I-8). Tests were made at Mach numbers from 0.60 to 1.20, with corresponding Reynolds numbers, based on the maximum diameter of the model, from 1.81 \times 10 6 to 3.52 \times 10 6 . The range of mean angle of attack was from 46 to 94 for configurations I-2C, I-2G, I-2F, and I-2, and from -2 $^{\circ}$ to 16 $^{\circ}$ for configuration I-8. The reduced-frequency parameter varied from 0.015 to 0.140. The amplitude of the forced oscillation was 2 $^{\circ}$.

Configurations I-2C, I-2G, I-2F, and I-2 generally exhibited oscillatory longitudinal stability except at the lower values of mean angle of attack at the higher Mach numbers. The addition of control surfaces to configurations I-2C and I-2 produced no significant changes in the oscillatory longitudinal stability parameter. Configuration I-8 was unstable for all test conditions. The damping in pitch was generally marginal or negative for configurations I-2C without control surfaces, I-2G, and I-2F for all test conditions and for configuration I-2 at the higher values of α . Positive damping was observed for configuration I-8 at all test conditions and for configuration I-2 at the lower values of α at the higher Mach numbers. Correlation was noted between the rate of change of damping in pitch with angle of attack and the rate of change of stability with angle of attack; large increases of negative damping were generally associated with even slight increases of stability.

^{*}Title, Unclassified.





INTRODUCTION

A research program is being conducted by the National Aeronautics and Space Administration to determine the aerodynamic characteristics of several low lift-drag ratio reentry bodies which may be suitable for manned space flight. As a part of this program the damping in pitch and the oscillatory longitudinal stability have been determined experimentally at transonic speeds for three axisymmetric high-drag bodies having different shoulder radii, a high-drag body of revolution having an asymmetric afterbody and a blunted cone. The static aerodynamic data for some of the configurations reported herein are presented in reference 1.

SYMBOLS

All aerodynamic data are presented with respect to the body system of axes with moments referred to the pitch oscillation centers shown in figure 1. The coefficients were nondimensionalized with respect to the reference length and area presented for each configuration in figure 1.

A	reference area, $\frac{\pi d^2}{4}$, sq ft
d	reference length, maximum body diameter, ft
М	free-stream Mach number
đ	pitching velocity, $\frac{\partial \theta}{\partial t}$, radians/sec
ģ	pitching acceleration, $\frac{\partial^2 \theta}{\partial t^2}$, radians/sec ²
R	Reynolds number based on d
t	time, sec
v	free-stream velocity, ft/sec
α	mean angle of attack, deg
å	time rate of change of angle of attack, $\frac{\partial \alpha}{\partial t}$, radians/sec



θ instantaneous angle of pitch, radian

$$\rho$$
 mass density of air, $\frac{1b-\sec^2}{ft^4}$

 ω 2 π (Frequency of oscillation), radians/sec

k reduced-frequency parameter, $\frac{\omega d}{V}$, radian

$$c_m$$
 pitching-moment coefficient, $\frac{\text{Pitching moment}}{\frac{\rho}{2}V^2\text{Ad}}$

$$C_{m_{\alpha}} = \frac{\partial C_{m}}{\partial \alpha}$$
 per radian

$$C_{m_{a}} = \frac{\partial C_{m}}{\partial \left(\frac{\dot{a}\dot{a}}{V}\right)}$$
 per radian

$$C_{mq} = \frac{\partial C_{m}}{\partial \left(\frac{qd}{V}\right)}$$
 per radian

$$C_{m_{\dot{q}}} = \frac{\partial C_{m}}{\partial \left(\frac{\dot{q}d^2}{v^2}\right)}$$
 per radian

 $C_{m_{ ilde{Q}}}$ + $C_{m_{ ilde{Q}}}$ damping-in-pitch parameter, per radian

 $c_{m_{\text{cl}}}$ - $k^2 c_{m_{\text{cl}}}$ oscillatory longitudinal stability parameter, per radian

MODELS AND APPARATUS

The five models used in this investigation consisted of three blunt axisymmetric bodies having ratios of shoulder radius to maximum model diameter of approximately 0.1 (configuration L-2C), approximately 0.048 (configuration L-2G), and 0 (configuration L-2F); a blunt body of revolution having an asymmetric afterbody (configuration L-2); and a blunted cone (configuration L-8). Dimensions of the models along with



the reference dimensions as used in the data reduction process are presented in figure 1. The models were constructed principally of fiber glass and Hetron, with control surfaces for configurations L-2C and L-2 made of magnesium.

The model surfaces exposed to the airstream were aerodynamically smooth and sufficiently hard to prevent surface erosion due to foreign particles in the airstream. The models had base openings for sting mounting on a mechanically driven single-degree-of-freedom forced-oscillation mechanism. The oscillation center for these tests is shown in figure 1. Configuration L-8 was oscillated about the pitch center corresponding to the proposed full-scale center-of-mass position. Because of tunnel power limitations, the model size of configurations L-2C, L-2G, L-2F, and L-2 was restricted and the center of oscillation of these models was located rearward of the proposed full-scale center-of-mass position. In order to provide a large angle-of-attack range for models other than L-8, the models could be mounted with wedge blocks which provided four different model angles with respect to the sting mechanism. With the available sting angle-of-attack range from -4° to 14°, the wedge blocks allowed a total model angle-of-attack range of 46° to 94°.

The forced-oscillation mechanism and the Langley 8-foot transonic pressure tunnel used for these tests are described in reference 2.

PROCEDURE AND TESTS

Dynamic data were obtained from the mechanically driven singledegree-of-freedom mechanism by alternating-current strain gages which sensed the instantaneous torque required to drive the model system and the instantaneous angular displacement of the model with respect to the These strain gages gave modulated 3,000-cycle outputs, which were passed through coupled electrical sine-cosine resolvers that rotated at the frequency of oscillation of the model. The resolvers divided the signals into orthogonal components, which were then demodulated and read on damped digital voltmeters. By responding only to signals at the fundamental frequency of oscillation, the resolver and damped-voltmeter system performs the desirable function of eliminating the effects of random torque inputs due to airstream turbulence. maximum torque required to drive the model, the maximum displacement of the model with respect to the sting, and the phase angle between the torque and displacement were found from the orthogonal components of torque and displacement. Since the frequency of oscillation was known, the system damping and the oscillatory spring-inertia characteristics could be computed. The measured wind-off characteristics were subtracted from the wind-on characteristics to give the desired aerodynamic



contribution. All data were taken with the model system oscillating near its resonant frequency, inasmuch as this condition results in greater accuracy in determining the system damping characteristics. A detailed discussion of this technique of measuring the dynamic stability characteristics of models is given in reference 3.

The tests were made at a tunnel stagnation pressure of 1 atmosphere at Mach numbers from 0.60 to 1.20, with corresponding Reynolds numbers, based on the maximum diameter of the model, from 1.81×10^6 to 3.52×10^6 . The range of mean angle of attack for each model corresponded to that anticipated for reentry. The angle-of-attack range (defined in a manner consistent with that used in ref. 1) was from 46° to 94° for all models except L-8, which had an angle-of-attack range from -2° to 16° . The reduced-frequency parameter varied from 0.015 to 0.140. The amplitude of the oscillation was 2° .

RESULTS AND DISCUSSION

The results of this investigation are presented as plots of the damping-in-pitch parameter $C_{m_{\hat{\mathbf{q}}}}+C_{m_{\hat{\mathbf{q}}}}$ and the oscillatory longitudinal stability parameter $C_{m_{\hat{\mathbf{q}}}}-k^2C_{m_{\hat{\mathbf{q}}}}$ as functions of mean angle of attack α in the following order:

Confi	gu	re	iti	Lor	1																									Figure
L-2C																								•						2(a)
L-2C,	W	it	h	c	ont	tro	ol	SI	ur.	fac	ces	3	٠	•					٠.				•	•		•	•			2(b)
L-2G			•		•		•	•	•		٠.				•	•				•	•	•	•			•				3 4
L-2			•	•	•	•	•						٠		•	•	•	•	٠	٠.		٠	•	٠			•	•		5(a)
L-2,	wi	tł	1 (cor	ıtı	ro.	L	su:	rfa	ace	es		•	•		•			•		٠	•			•	•	•		•	5(b)
L-8													٠.		٠															6

Different test-point symbols are used to indicate the portion of the α range obtained with different sting-model orientations. Positive values of $c_{m_{\mbox{\scriptsize q}}}+c_{m_{\mbox{\scriptsize \'e}}}$ indicate negative damping and positive values of $c_{m_{\mbox{\scriptsize q}}}-k^2c_{m_{\mbox{\scriptsize \'e}}}$ indicate oscillatory instability.

As noted in the section "Models and Apparatus," except for configuration L-8 the center of oscillation did not correspond to the proposed full-scale center-of-mass location. Results of previous tests, such as those of reference 4, have shown that changing the axial



location of the center of oscillation has little effect on the damping in pitch for short bodies similar to those tested in this program. The expected symmetry of the data about $\alpha=90^\circ$ for configurations L-2C, L-2G, and L-2F is in some cases difficult to detect. Had data been taken to higher angles of attack, the peaks in the data indicated at mean angles of attack between 80° and 90° would be expected to occur between 90° and 100° , giving symmetry to the data about $\alpha=90^\circ$. It is noted that the data often show symmetry about angles of attack slightly greater than 90° . Because of the range of angle of attack, the base openings were not symmetrical, as can be seen in figure 1. In addition, at $\alpha=90^\circ$ the models were mounted on a 10° wedge block (see the section "Models and Apparatus"); this mounting resulted in an angle of 10° between the sting and the model center line. These two conditions probably account for the tendency for symmetry in the data to occur slightly above $\alpha=90^\circ$.

Configuration L-2C exhibited oscillatory longitudinal stability for all test conditions (fig. 2(a)). Configuration L-2G (fig. 3) was unstable at $\alpha=46^{\circ}$ and M = 1.20 with reduced variation of stability with α compared with that observed at the low Mach numbers for L-2C (fig. 2(a)). Configuration L-2F had additional instability at the lower values of α for the higher Mach numbers (fig. 4). These increases in instability with changes in configuration from L-2C to L-2F are probably due to increased areas of attached flow behind the leading segment of the shoulder. In regions where the stability changed gradually with α , the damping for configurations L-2C, L-2G, and L-2F was essentially zero. However, abrupt changes in stability with α were always accompanied by abrupt changes in damping. An increase in stability with increasing α is accompanied by a decrease in positive damping.

The addition of control surfaces to L-2C (fig. 2(b)) increased the level of stability and introduced variations in stability with α at the higher Mach numbers that were not present when the control surfaces were off. These variations in stability were again accompanied by variations in aerodynamic damping.

Configuration L-2 without control surfaces was stable for values of α above 60° at all Mach numbers (fig. 5(a)). At the lower values of α , marked instability occurred. The abrupt variation of oscillatory stability with α is again accompanied by abrupt changes in the damping. The addition of the control surfaces to L-2 (fig. 5(b)) produced small changes in the stability and damping characteristics at all test conditions.

Configuration L-8 (fig. 6) was unstable but had positive damping for all test conditions.





Reentry configurations L-2C, L-2G, L-2F, and L-2 generally exhibited oscillatory longitudinal stability, except at the lower values of mean angle of attack at the higher Mach numbers. The addition of control surfaces to configurations L-2C and L-2 produced no significant changes in the oscillatory longitudinal stability parameter. Configuration L-8 was unstable for all test conditions.

The damping in pitch for configurations L-2C, L-2G, and L-2F for all test conditions, and for configuration L-2 at the higher values of α was generally marginal or negative. Positive damping was observed for configuration L-8 at all test conditions and for configuration L-2 at the lower values of α at the higher Mach numbers.

Correlation was noted between the rate of change of damping in pitch with angle of attack and the rate of change of stability with angle of attack; large increases of negative damping were generally associated even with slight increases of stability.

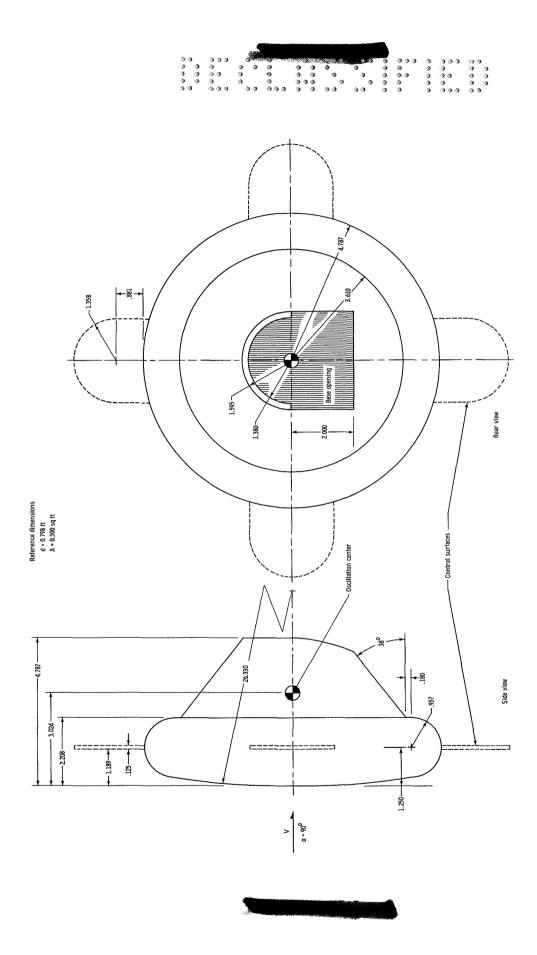
Langley Research Center,
National Aeronautics and Space Administration,
Langley Air Force Base, Va., August 25, 1961.





- 1. Rainey, Robert W., compiler: Summary of Aerodynamic Characteristics of Low-Lift-Drag-Ratio Reentry Vehicles From Subsonic to Hypersonic Speeds. NASA TM X-588, 1961.
- 2. Bielat, Ralph P., and Wiley, Harleth G.: Dynamic Longitudinal and Directional Stability Derivatives for a 45° Sweptback-Wing Airplane Model at Transonic Speeds. NASA TM X-39, 1959.
- 3. Braslow, Albert L., Wiley, Harleth G., and Lee, Cullen Q.: Dynamic Directional Stability Derivatives for a 45° Swept-Wing-Vertical-Tail Airplane Model at Transonic Speeds and Angles of Attack, With a Description of the Mechanism and Instrumentation Employed. NACA RM L58A28, 1958.
- 4. Beam, Benjamin H., and Hedstrom, C. Ernest: The Damping in Pitch of Bluff Bodies of Revolution at Mach Numbers from 2.5 to 3.5. NASA TM X-90, 1959.

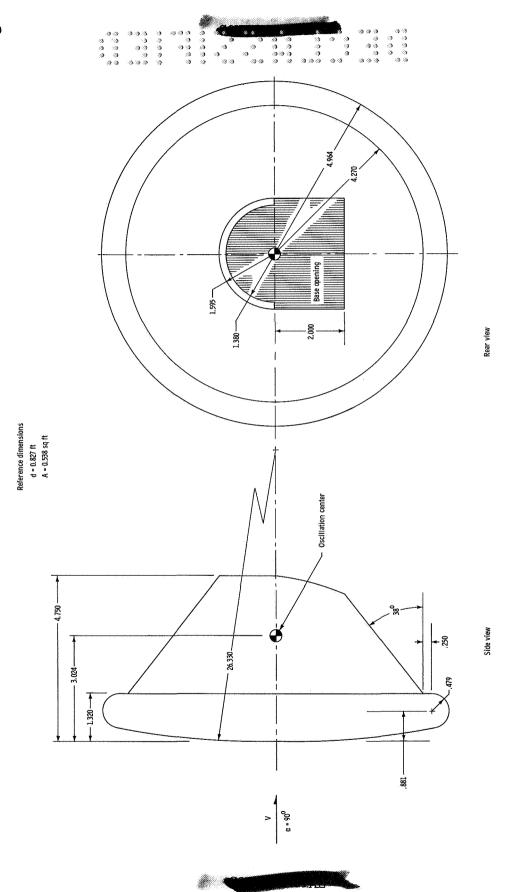




L-1642

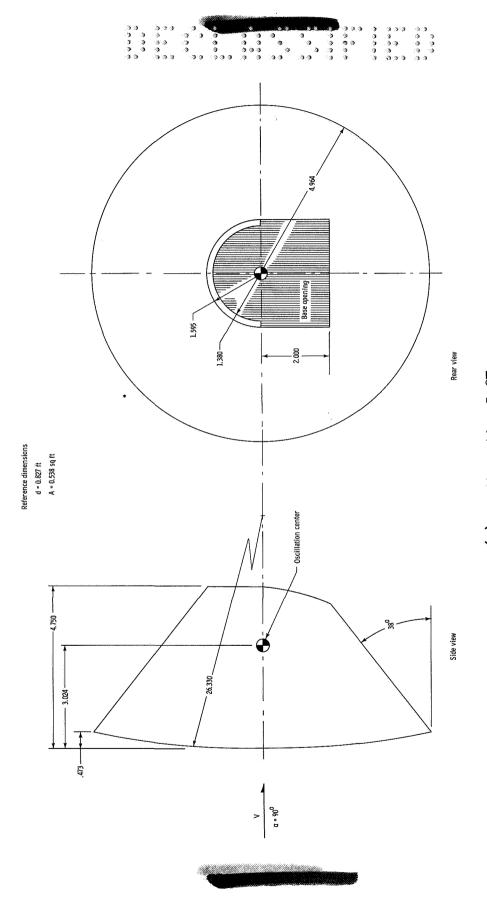
Figure 1.- Sketch of the models showing design dimensions and the angle-of-attack convention. All linear dimensions are in inches.

(a) Configuration L-2C.



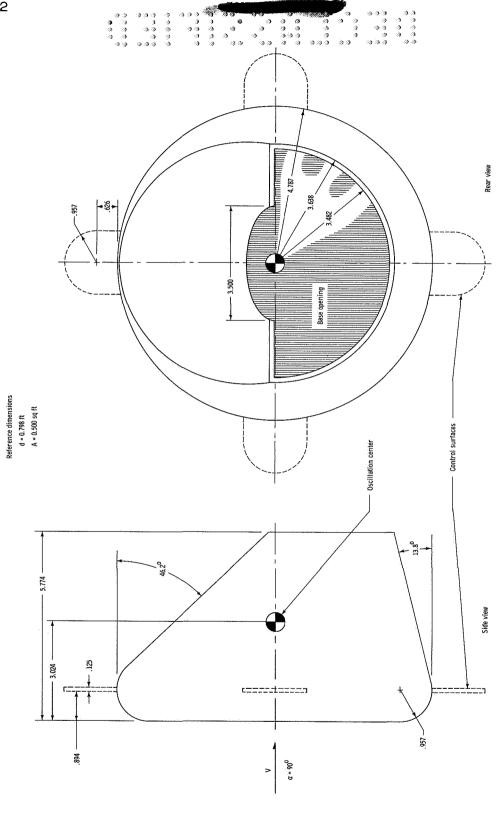
(b) Configuration L-2G.

Figure 1.- Continued.



(c) Configuration L-2F.

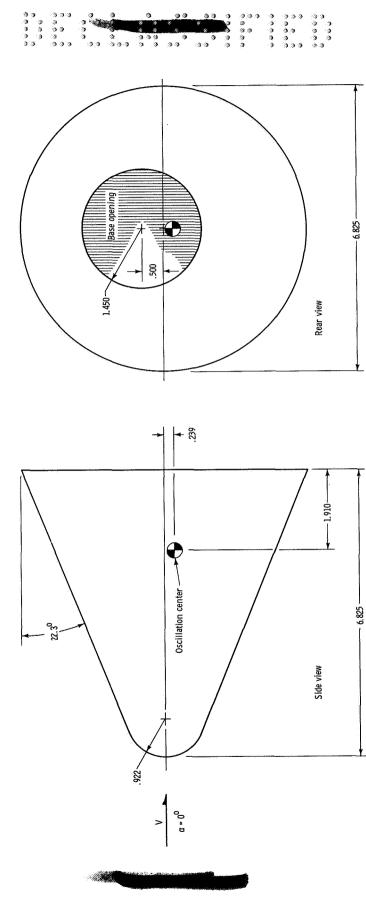
Figure 1.- Continued.



(d) Configuration L-2.

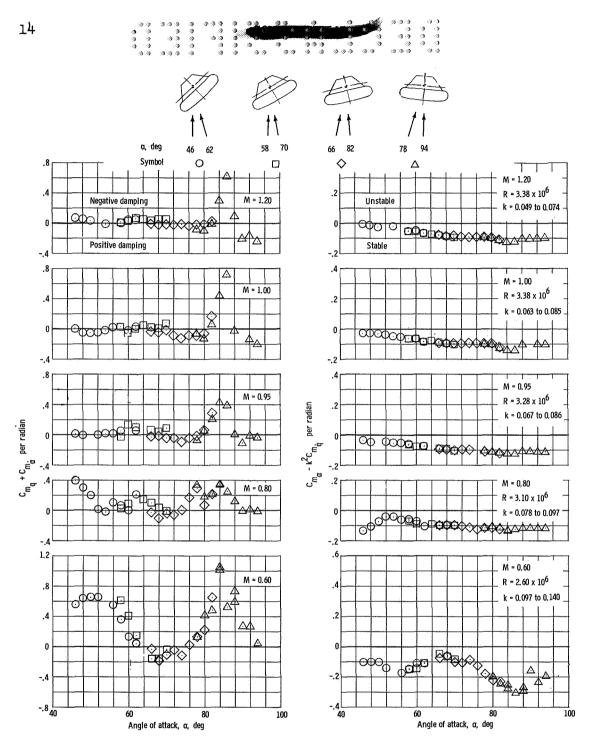
Figure 1.- Continued.

Reference dimensions d = 0.569 ft A = 0.254 sq ft



(e) Configuration L-8.

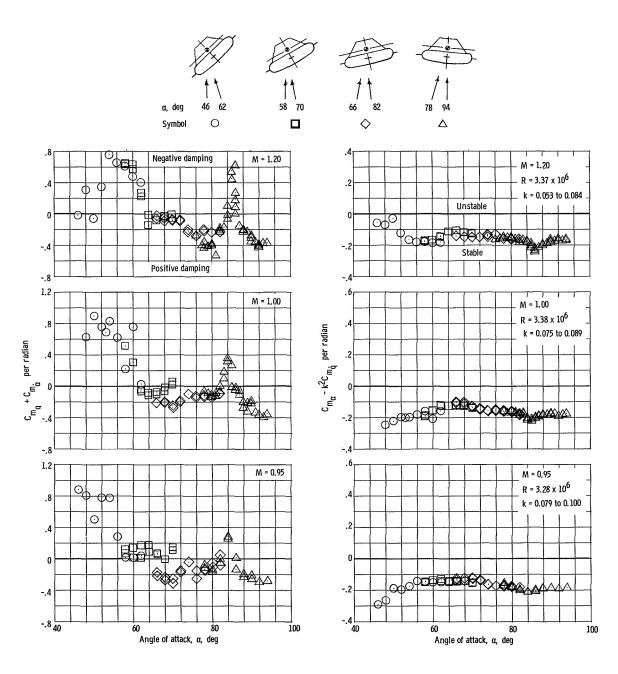
Figure 1.- Concluded.



(a) Configuration L-2C.

Figure 2.- The damping-in-pitch parameter $C_{m_{\mathbf{q}}} + C_{m_{\mathbf{\dot{q}}}}$ and the oscillatory longitudinal stability parameter $C_{m_{\mathbf{q}}} - k^2 C_{m_{\mathbf{\dot{q}}}}$ as functions of mean angle of attack.

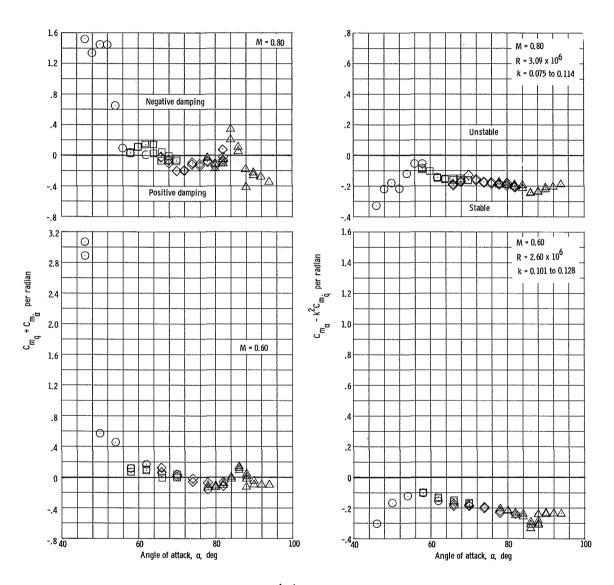




(b) Configuration L-2C, with control surfaces.

Figure 2.- Continued.





(b) Concluded.

Figure 2.- Concluded.



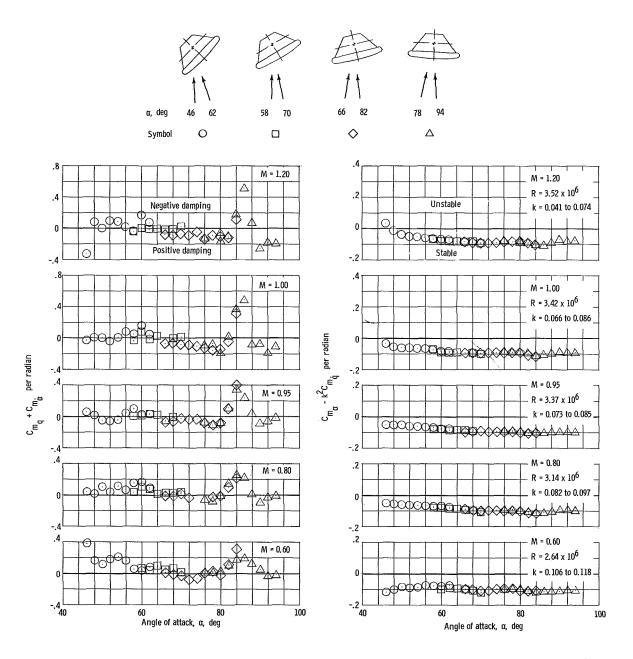


Figure 3.- The damping-in-pitch parameter $C_{m_{\mathbf{q}}} + C_{m_{\dot{\alpha}}}$ and the oscillatory longitudinal stability parameter $C_{m_{\alpha}} - k^2 C_{m_{\dot{\mathbf{q}}}}$ as functions of mean angle of attack for configuration L-2G.



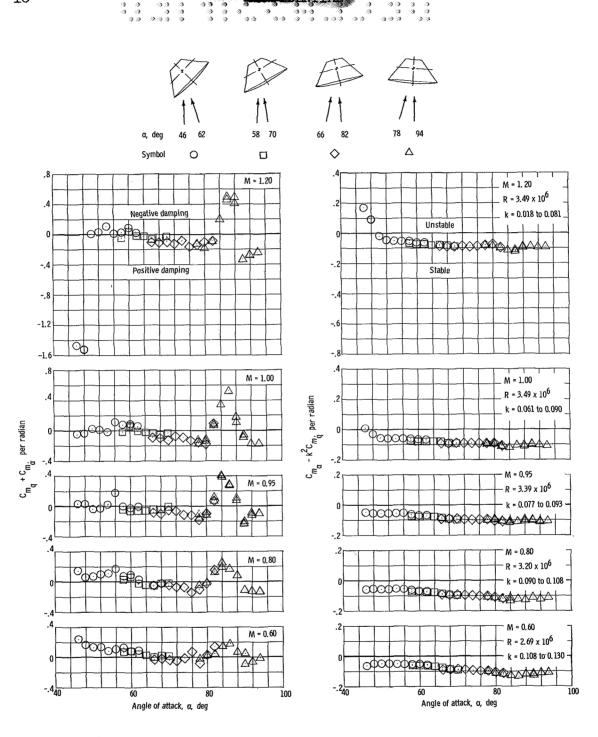
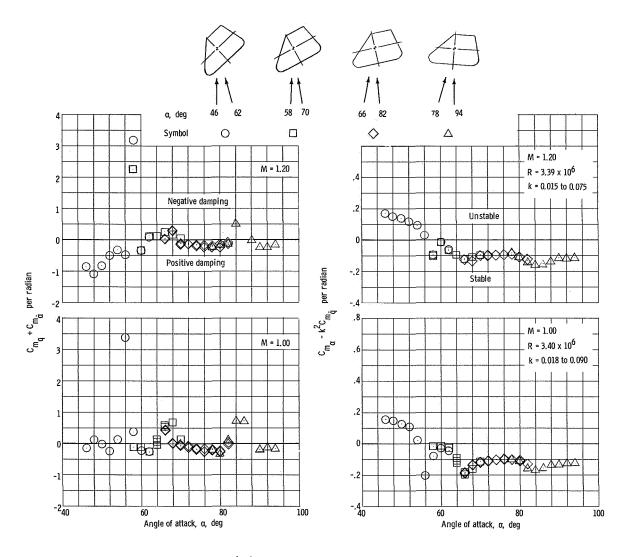


Figure 4.- The damping-in-pitch parameter $C_{m_{\mathbf{Q}}} + C_{m_{\mathbf{C}}}$ and the oscillatory longitudinal stability parameter $C_{m_{\mathbf{C}}} - k^2 C_{m_{\mathbf{Q}}}$ as functions of mean angle of attack for configuration L-2F.





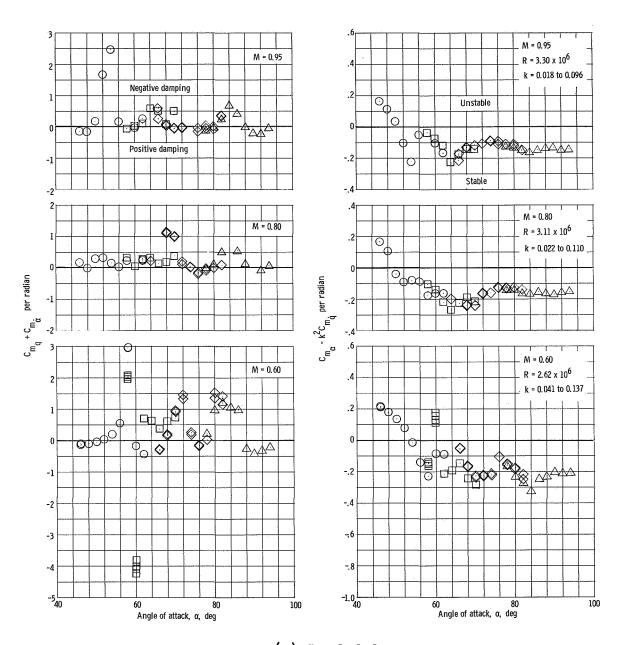


(a) Configuration L-2.

Figure 5.- The damping-in-pitch parameter $C_{m_{\bf q}}+C_{m_{\bf \tilde{\alpha}}}$ and the oscillatory longitudinal stability parameter $C_{m_{\bf q}}-k^2C_{m_{\bf \tilde{q}}}$ as functions of mean angle of attack.





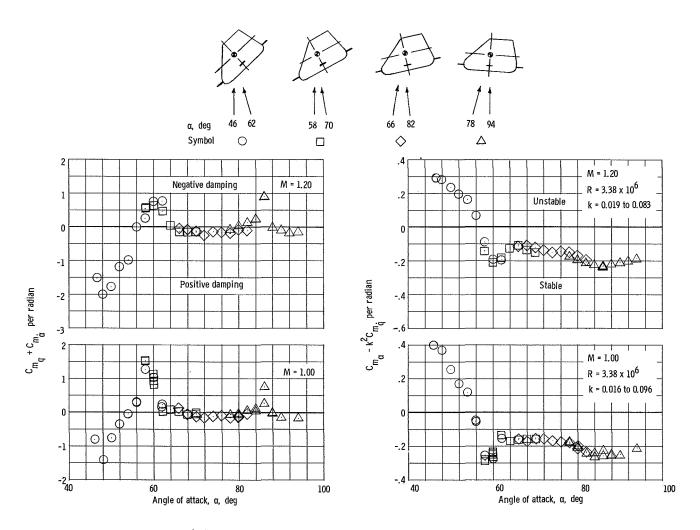


(a) Concluded.

Figure 5.- Continued.





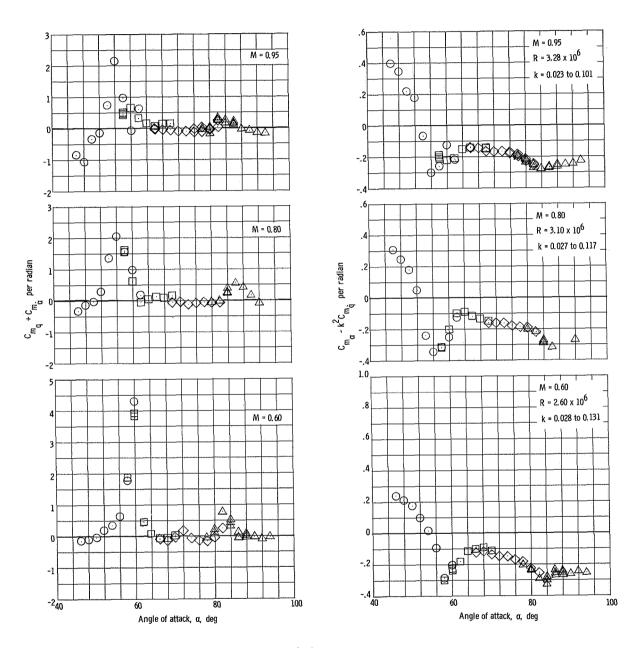


(b) Configuration L-2, with control surfaces.

Figure 5.- Continued.







(b) Concluded.

Figure 5.- Concluded.



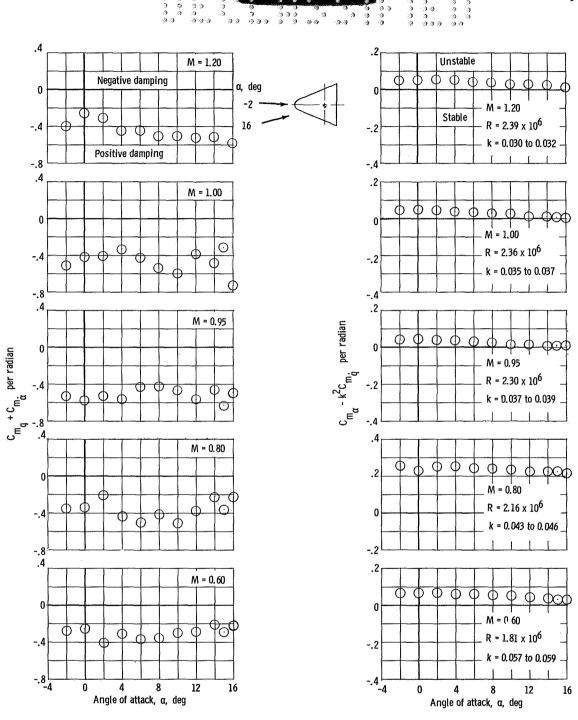


Figure 6.- The damping-in-pitch parameter $c_{m_{\hat{\mathbf{q}}}} + c_{m_{\hat{\mathbf{c}}}}$ and the oscillatory longitudinal stability parameter $c_{m_{\hat{\mathbf{q}}}} - k^2 c_{m_{\hat{\mathbf{q}}}}$ as functions of mean angle of attack for configuration L-8.

39/39	333	3	1000	43	0.4		5 ° 6.	o de de Care	1000	ைற	3 3	
9 9	()	· 😘	- 3	3"		. 9	9 69.	* 4	6 0	-3	ಾ	
3 3	ூற	- 3	3 3	-3	9	- 😘	9 8	- 3	- 13	0.0		
3 3	•	3	9	ಿ	3	-33	333	€	()	- 3	3	
(A) (A)	333	3	3	ಾ	(3) (3)	39.3	3 3	O.O.O.	00	300	ഭ	